Millennial-scale vegetation changes in the tropical Andes using ecological grouping and ordination methods

Dunia H. Urrego (1), Henry Hooghiemstra (2), Oscar Rama-Corredor (3), Belen Martrat (3), Joan O. Grimalt (3), Lonnie Thompson (4), Mark B. Bush (5), Zaire González-Carranza (2), Jennifer Hanselman (6), Bryan Valencia (5), César Velásquez-Ruiz (7).

(1) Geography, College of Life and Environmental Sciences, University of Exeter, United Kingdom.
(2) Institute for Biodiversity and Ecosystem Dynamics, University of Amsterdam, The Netherlands.
(3) Department of Environmental Chemistry, IDAEA-CSIC, Spain.
(4) School of Earth Sciences and Byrd Polar and Climate Research Center, The Ohio State University, USA.
(5) Department of Biological Sciences, Florida Institute of Technology, USA.
(6) Department of Biology, Westfield State University, USA.
(7) Bio-Science School, Universidad Nacional de Colombia, Colombia.

Prepared for publication in: Climate of the Past
Track record of manuscript: 29 April 2013 skeleton text by HH **version-1;** August 2013, added notes on methods, key questions and results DHU; 17 July 2014 **version-2** by DH Urrego; 22-23 July HH; 5Sep **version-4** by DHU; 9Sept HH input; 17thOct **version-6** by DHU; HH input 20Oct-4Nov; **version-7** by DHU 21Nov2014; 1Dec2014 LT, OR-C and BM input; HH input 30Nov-3Dec; **version-8** by DHU 23Jan15. HH input 26Jan15. BM input 28Jan15. **Version-9** by DHU 29Jan2015. BM feedback 30Jan. **Submission**: 31 Jan 2015 (**version-10**). Reviews May-July 2015. HH input 5Nov2015. Revised manuscript **version-11 by DHU** on 2-4Dec 2015. LT input 7Dec2015. Revised submission: 8 Dec 2015 (**version-12**).
Accepted for publication: 27 January 2016.

Abstract

We compare eight pollen records reflecting climatic and environmental change from northern and southern sites in the tropical Andes. Our analysis focuses on the last 30,000 years, with particular emphasis on the Pleistocene to Holocene transition. We explore ecological grouping and downcore ordination results as two approaches for extracting environmental variability from pollen records. We also use the records of aquatic and shoreline vegetation as markers for lake level fluctuations, and moisture

availability. Our analysis focuses on the signature of millennial-scale climate variability in the tropical Andes, in particular, Heinrich stadials (HS) and Greenland interstadials (GI).

The pollen records show an overall warming trend during the Pleistocene-Holocene transition, but the onset of post-glacial warming differs in timing among records. We identify rapid responses of the tropical vegetation to millennial-scale climate variability. The signature of HS and the Younger Dryas are generally recorded as downslope Upper Forest Line (UFL) migrations in our transect, and are likely linked to air temperature cooling. The GI1 signal is overall comparable between northern and southern records and indicates upslope UFL migrations and warming in the tropical Andes. Our marker for lake level changes indicated a north to south difference that could be related to moisture availability. The air temperature signature recorded by the Andean vegetation was consistent with millennial-scale cryosphere and sea surface temperature changes, but suggests a potential difference between the magnitude of temperature change in the ocean and the atmosphere. We also show that AP% and DCA scores are two complementary approaches to extract environmental variability from pollen records.

Keywords: arboreal pollen sum, detrended correspondence analysis, millennial-scale climate variability, pollen records, tropical Andes

1. Introduction

The signature of millennial-scale climate variations is recorded in ice cores, and in marine and terrestrial sediment archives both in the northern and southern hemispheres (NGRIPmembers, 2004; EPICA, 2006; Baker et al., 2001; Harrison and Sanchez Goñi, 2010; Hessler et al., 2010). The clearest manifestations of millennial-scale climate events are observed in Greenland ice core records (Wolff et al., 2010) and North-Atlantic marine sequences (Sánchez Goñi and Harrison, 2010). The Greenland interstadials (GI) are characterised by rapid warming in ice core records and can last up to 2500 years (Wolff et al., 2010). A second type of millennial-scale climate events are the Heinrich events (HE) (Heinrich, 1988), which are marked by an abrupt increase in the proportion of ice-rafted debris (IRD) from iceberg discharges in the Ruddiman Belt (Ruddiman, 2001). These iceberg discharges deliver fresh water into the North Atlantic and disrupt the Atlantic Meridional Overturning Circulation (Hemming, 2004) resulting in global climate changes. The intervals associated with North-Atlantic iceberg discharges are termed Heinrich Stadials (HS) (Sánchez Goñi and Harrison, 2010) and have been linked to temperature and precipitation changes in other regions of the world.

The signature of millennial-scale climate variability in the American tropics has mostly been linked to precipitation change, specifically to southward migrations of the Intertropical Convergence Zone (ITCZ) and variations in the strength of monsoonal systems during HS. Model simulations and climate reconstructions suggest that HS result in a southward shift of the thermal equator and the ITCZ (Broccoli et al., 2006) linked to decreased sea surface temperature (SST) in the North Atlantic and increased SST in the South Atlantic. Such an atmospheric and oceanic configuration is associated with a weakened North-American Monsoon (Lachniet et al., 2013), and reduced precipitation in central (Escobar et al., 2012) and northern South America (Peterson et al., 2000). The precipitation signature of HS is also described as wet episodes in the Bolivian Altiplano (Baker et al., 2001; Fritz et al., 2010) and as enhanced South American summer monsoon (SASM) activity in southeastern Brazil (Cruz et al., 2005). In the Ecuadorian Amazon, precipitation change appears to be positively correlated with some HS (Mosblech et al., 2012).

GI have also been linked to precipitation changes in the American tropics. These include wet conditions during GI1 in Central America (Escobar et al., 2012) and decreased run-off in the Guyana Basin (Arz et al., 1998). Some GI appear to be associated with reduced lake levels in western Amazonia (Urrego et al., 2010) and decreased humidity in the Bolivian Altiplano (Baker et al., 2001). Weakening of SASM and reduced precipitation are also associated with the onset of some GI in speleothem records from subtropical Brazil (Cruz et al., 2005). The precipitation signals of HS and GI indicate that climatic conditions in the American tropics were far from stable during these millennial-scale climate events.

Estimates of temperature change during HS and GI in the tropics differ in magnitude and are hindered by the number of available records. The magnitude of tropical Atlantic SST warming at the onset of GI1 for instance is estimated to be less than 1°C in the Tobago Basin (Rühlemann et al., 2003), 2°C in the Colombian basin (Schmidt et al., 2004) and 3.8°C in the Guyana Basin (Rama-Corredor et al., 2015). The isotopic record from the Sajama ice core also indicates a large-magnitude change during GI1 that has been linked to precipitation but could also be associated with air temperature warming (Thompson et al., 1998). In the Colombian Andes, the best resolution vegetation-based reconstruction of air temperatures available to date suggests that the magnitude of warming associated with GI1 is as large as 9°C (Groot et al., 2011), twice the SST estimate. Similarly, the signature of HS in the same record suggests downslope forest migrations and large-magnitude temperature depressions (Bogotá et al., 2011). A

regional synthesis suggests that the vegetation signature of HS and GI can be opposite between the northern and southern parts of the region influenced by the ITCZ (Hessler et al., 2010) and highlights the paucity of records. Overall, whether there is a consistent air and ocean temperature signature of millennial-scale climate events in the American tropics remains unclear.

The main objective of this paper is to assess the signature of millennial-scale climate variability in the tropical Andes, and to test whether it is consistent among northern and southern sites. We re-analyse a suite of eight pollen records that reveal vegetation changes at mid to high-elevations during last the 30,000 years BP (ka), with particular emphasis on the Pleistocene to Holocene transition. We compare all records on a common timescale, and explore how records expressed as percentage data and as downcore detrended correspondence analysis (DCA) time series can provide different information on environmental change. This study differs from previous studies that have focused on vegetation changes and their palaeoecological meaning. Here, we use the Andean vegetation as a marker for climatic change. We consider vegetation change as one of the internal responses of the climate system and integrate our observations with records that reveal the responses of the cryosphere and the ocean to millennial-scale climate variability in the American tropics.

2. Environmental setting: vegetation and climate

Vegetation in the north and central Andes is dominated by lower montane forest above 1000 m elevation and up to c. 2300 m where there is absence of night frost. Upper montane forests are found where night frost may occur and extend up to the upper forest line (UFL). The UFL position, defined as the highest contour of continuous forest (Bakker et al., 2008), is instrumental in temperature reconstructions as it coincides with the c. 9.5°C mean annual temperature (Hooghiemstra, 1984). The UFL is found in the study area between 3200 and 3500 m elevation and depends amongst other factors on regional temperature, precipitation, ground-level cloudiness, and soil conditions. In the northern Andes of Colombia and Ecuador relatively humid Páramo (Luteyn and Churchill, 1999) is found between the UFL and the perennial snow at c. 4800 m. Much drier Puna vegetation occurs above the UFL in Perú and Bolivia. The Huancabamba Deflection (Weigend, 2002), a low elevation part of the Andes between Ecuador and Perú, forms the transition between wet Páramo and dry Puna.

Topography is a key environmental variable in the tropical Andes (Graham, 2009). It determines air temperature change (Vuille and Bradley, 2000), and precipitation variability and spatial distribution (Garreaud et al., 2009). Air temperature decreases with

elevation, with modern empirically derived lapse rates of 5.5°C per 1000 m (Bush et al., 2004). Air temperature in the tropical Andes can also be significantly reduced by cold-air advection funnelled through Andean valleys from the northern (Poveda et al., 2006) and southern (Garreaud, 2000) high latitudes. Cold fronts also affect precipitation regimes due to convective cloudiness (Poveda et al., 2006; Garreaud et al., 2009). In particular, southern-hemisphere cold fronts have been linked to ca. 30% of summertime precipitation in western Amazonia (Garreaud and Wallace, 1998).

With respect to precipitation distribution, spatial differences between the eastern and western Andean flanks are partly due to topography (Poveda et al., 2011). Moisture on the eastern flank is primarily sourced in the tropical Atlantic and Amazonia, while SST in the tropical Pacific modulates precipitation on the western flank (Vuille and Bradley, 2000). On the eastern flank, the Andean mountains form a barrier to moisture, and the altitudinal temperature decline forces that humidity to condense and form clouds (Poveda et al., 2006). In areas of the eastern flank where prevailing winds and topography are not favourable, cloud cover can be low and precipitation can be less than 1500 mm, forming relatively dry enclaves (Killeen et al., 2007). In contrast, moisture regimes on the western flank are linked to the westerly Chocó jet in the northern Andes (Poveda et al., 2006), and to upwelling and El Niño Southern Oscillation (ENSO) in the central and southern Andes (Vuille et al., 2000). Such a difference in moisture drivers results in a large precipitation gradient from north to south, with some of the rainiest areas on earth found on the Pacific coast of Colombia, and deserts found along the Peruvian coast. Rain shadow effects govern rainfall in inter-Andean valleys (Vuille et al., 2000).

Several large-scale atmospheric and oceanic mechanisms modulate precipitation regimes in the tropical Andes (Fig. 1). The position of the ITCZ is primarily forced by trade wind convergence and Atlantic and Pacific SSTs, and is linked to continental rainfall and seasonality at sub-annual timescales (Garreaud et al., 2009; Poveda and Mesa, 1997). At inter-annual to millennial timescales, the inter-hemispheric migration of the ITCZ seems to respond to multiple factors including insolation and the position of the thermal equator (Fu et al., 2001), high-latitude temperatures and land-sea ice extent (Chiang and Bitz, 2005), and high-latitude North Atlantic variability (Hughen et al., 1996). The ITCZ is in turn linked to the distribution of mesoscale convective systems in northwestern South America, contributing an average of 70% of annual precipitation in the region (Poveda et al., 2006).

The SASM (Fig. 1) is linked to a large area of precipitation and convection that forms over most of Amazonia and subtropical Brazil during the austral summer

(Garreaud et al., 2009). This low pressure system delivers a large proportion of annual rainfall between December and February (Garreaud et al., 2009), and isotopic fingerprinting suggests that the tropical Atlantic is its main moisture source (Vuille and Werner, 2005). This moisture is transported across Amazonia by easterly trade winds (Vuille et al., 2000) and is linked to the South American low-level jet (SALLJ) (Zhou and Lau, 1998). Variations in the position of the Atlantic ITCZ are suggested to play a role in modulating the strength of the SASM on interannual to decadal timescales (Zhou and Lau, 1998). SASM strength has also been linked to the mean state of the Pacific (Vuille and Werner, 2005), and interannual and long-term ENSO variability (Zhou and Lau, 1998).

ENSO drives a large portion of the interannual precipitation variability in the tropical Andes, despite regional differences in timing, magnitude and direction of change (Poveda et al., 2011). Warm ENSO events are associated with decreased rainfall and more prolonged dry seasons in the Colombian Andes (Poveda et al., 2006). Drought is also experienced in northeast Brazil during warm ENSO events, while southern Brazil and the Ecuadorian Pacific coast experience increased rainfall (Zhou and Lau, 2001). Warm ENSO events are also associated with strengthening of the SALLJ along the eastern flank of the Andes, and enhancement of the SASM (Zhou and Lau, 2001).

3. Methods

We use eight pollen records from the tropical Andes to reconstruct environmental change at a regional scale over the past 30 ka (Fig. 1, Table 1). This temporal focus is driven by the time span of available records. Selected lakes form a north-to-south transect from 6°N to 16°S and lie at mid- (<3000 m) and high-elevations (>3000 m) in the tropical Andes. For the purpose of this paper, sites are classified according to their latitudinal position into northern (latitude north), central (latitude < 10ºS) and southern (latitude > 10ºS) Andean sites (Table 1). The sites are located in inter-Andean valleys partly lying in the rain shadow, the eastern flank of the Andes facing the Amazon lowlands, and the Peruvian-Bolivian Altiplano (Table 1). This latitudinal transect provides a large environmental gradient and includes sites with various moisture sources. In the two northernmost Colombian sites, the Atlantic ITCZ and ENSO modulate moisture (Velásquez and Hooghiemstra, 2013; Bogotá et al., 2011). Further south, Lakes La Cocha and Surucucho are located on the eastern flank of the Andes and receive most precipitation from Amazonian orographic rains (Colinvaux et al., 1997; González-Carranza et al., 2012). Lakes Chochos, Pacucha and Consuelo lie on the eastern flank of

the Andes, and Lake Titicaca on the Peruvian/Bolivian Altiplano. Lake Chochos precipitation is sourced from Amazonian convection and the SASM (Bush et al., 2005). The SASM also is the primary moisture source for Lakes Pacucha, Consuelo and Titicaca (Urrego et al., 2010; Valencia et al., 2010; Baker et al., 2001) (Table 1).

We selected pollen records where knowledge of regional vegetation was sufficient to allow a classification of pollen taxa into ecological groups. The selected records also met minimum requirements of stratigraphic consistency and chronology quality. We used records in which stratigraphic consistency allowed linear interpolations between radiocarbon-dated samples (Table 1). We also selected records that included in average 5 radiocarbon ages in 10 ka. Age models developed by the original authors were used, except for Llano Grande. For this record, we took the radiocarbon dates available in the original publication and generated a linear interpolated age model based on calibrated ages using Calib 7.1, IntCal13 (Reimer et al., 2013). The temporal resolution of the records ranged from an average of ca. 26 years in La Cocha to 530 years in one of the sequences from Lake Titicaca (Table 1). Given the differences in temporal resolution among records, we only discuss major trends and refrain from drawing conclusions beyond the chronological constraints of each record.

To assess the regional signature of millennial-scale climate events, our analysis benefits from comparisons with direct proxies of tropical Atlantic SST from MD03-2616 (7°N, Guiana basin), and isotopic records from the Sajama ice cap (18°S). We explore the degree of consistency between these independent markers and changes recorded by the Andean vegetation as far as the chronological uncertainties allow.

Protocol to extract environmental information from pollen records

Raw pollen counts were obtained from the original authors or from the Latin American pollen database (http://www.ncdc.noaa.gov/paleo/lapd.html). We calculated a pollen sum that included only terrestrial taxa, and re-calculated pollen percentages of individual taxa based on that sum. The ecological grouping of terrestrial taxa was based on the ecological information published by the original authors. For sites where this information was unavailable, we followed the author's interpretations of the pollen record, ecological knowledge of the regional vegetation, and information from modern pollen calibrations (Reese and Liu, 2005; Urrego et al., 2011; Weng et al., 2004). We considered that ecological envelopes of Andean taxa at genus level may be wide, as more than one species may be reflected in one pollen taxon. We also took into account that the ecological affinity of a pollen taxon in a relatively dry inter-Andean valley may differ from that of the same taxon in a humid cloud forest. Our interpretations of fossil pollen

252 spectra into past climate change included region-specific conditions. For example,
253 presence of pollen of Cactaceae and *Dodonaea* reflected local rain shadow effects, rather
254 than regional dry climates. Rare pollen taxa with unknown ecological affinity were
255 excluded from this classification.
256 Ecological groups include Puna (or Páramo), subpuna (or subpáramo), Andean
257 (upper montane) forest, sub-Andean (lower montane) forest, and taxa from tropical
258 lowland vegetation. The Puna (relatively dry) and Páramo (relatively wet) groups include
259 taxa from cold vegetation above the UFL (Bakker et al., 2008; Groot et al., 2011). These
260 groups also include transitional taxa between the UFL and Puna or Páramo. The Andean
261 and sub-Andean groups reflect high-elevation and mid-elevation forests found today
262 between ca. 1200 and 3200-3500 m elevation. Finally, tropical lowland taxa reflected
263 warm and moist forests below ca. 1200 m elevation.
264 The arboreal pollen percentage (AP%) groups the regional vegetation for each site.
265 Interpretation of AP% is dependent on the altitudinal location of a given site relative to
266 the modern UFL (Hooghiemstra and van der Hammen, 2004). For instance, in Lake
267 Fúquene at 2540 m, AP% includes Andean and sub-Andean taxa. In Llano Grande at
268 3650 m, AP% only includes cold Andean taxa as pollen grains from sub-Andean forests
269 hardly reach this high-elevation site. AP% is most sensitive when sites are located
270 between the highest interglacial and the lowest glacial UFL positions. We therefore
271 anticipate a lower sensitivity of the records from Lake Consuelo (1360 m) and Lake
272 Titicaca (3800 m) as a consequence of site location. Using the ecotone of the upper/lower
273 montane forest is not feasible yet as this ecotone is palynologically insufficiently
274 constrained (Hooghiemstra et al., 2012). Changes in AP% relate to altitudinal migrations
275 of montane vegetation and the relative position of the UFL, an ecological boundary
276 relatively well established in climatological terms (Körner, 2007; Hooghiemstra, 2012).
277 The terrestrial pollen sum excludes taxa of the aquatic and shoreline vegetation,
278 such as Cyperaceae, *Isöetes*, *Myriophyllum* and other taxa described by original authors
279 as aquatic and wet shoreline elements. We have followed the shoreline vegetation
280 zonation detailed by González-Carranza et al. (2012), when information on aquatic
281 vegetation was unavailable. We establish an "aquatic pollen sum" that includes taxa
282 grouped into shoreline, shallow- and deep-water taxa, reflecting a gradient of water
283 depth. The shoreline group includes taxa found in the wet and seasonally flooded shores
284 (i.e. *Plantago*, *Rumex* and *Typha*), shallow water taxa are found growing up to 1 m water
285 depth (i.e. *Hydrocotyle* and *Ranunculus*), and deep water taxa include *Isöetes* ferns and
286 other aquatic plants found up to 6 m water depth (González-Carranza et al., 2012). We
287 calculate a ratio (D/SS) between taxa characteristic of deep water over taxa growing in

shallow water and wet shores, and use it as an indicator of lake level changes and moisture availability. D/SS is based on the sum of aquatic taxa and is independent of AP%.

Two DCA analyses (McCune and Grace, 2002) were performed on untransformed terrestrial pollen percentages for each site. The first DCA was run on the entire pollen percentage matrices. A second DCA was run on reduced pollen percentage matrices after applying a filter that aimed to eliminate noise caused by rare pollen taxa (Birks and Birks, 1980). This filter retained taxa with at least 1% abundance and that were found in at least 5 samples per record. Taxa that met only the latter requirement, but had abundances below 1% were retained as such taxa likely reflected low pollen producers. Iterations were run until a stable solution was reached for all ordinations. To make DCA scores comparable between records, axis scores were standardized by calculating z-scores based on the mean and standard deviation for each record. Rates of ecological changes (RoC) were calculated as the dissimilarity distance between two consecutive pollen time slices divided by the time interval in between (Urrego et al., 2009). Euclidean, Sorensen and Bray Curtis dissimilarity distances (McCune and Grace, 2002) were calculated based on raw pollen percentages. The DCA axis scores for the first four axes were also used to calculate RoC using a Euclidean distance. RoC calculated using raw percentages were compared with RoC based on DCA axis scores to evaluate the influence of DCA variance reduction.

4. Results and interpretation

The proportions of sub-Andean (lower montane) and Andean (upper montane) forest taxa vs. vegetation located above the UFL (Puna and Páramo) show temporal variations that appear synchronous among some sites (Fig. 2). The comparison of AP% vs. DCA1 z-scores demonstrates similar trends in three of the eight pollen records analysed (Fig. 3). In the remaining five records, AP% and DCA z-scores trends differ in at least part of the record, despite a few similarities. The record of D/SS potentially reflects lake level changes and moisture availability that appear to be registered at most studied sites (Fig. 4). In the following section we describe results from our re-analysis of each of eight selected pollen records.

4.1 Llano Grande (Velásquez and Hooghiemstra, 2013)

The Llano Grande site is located near the current position of the UFL at 3650 m elevation. Changes in AP% at this elevation are expected to be sensitive to changes in the composition of the Andean forests found downslope today. The trends of DCA1 z-scores

(reversed) and AP% are remarkably similar (Fig. 3) suggesting that temperature, the driver of changes in AP%, is also the strongest driver of DCA1. The abundance of Andean taxa (AP%) shows a trough between ca. 12.5 and 10.5 ka (Fig. 2 and 3). Several AP% oscillations are observed during the Holocene. D/SS shows a peak after the onset of the pollen record at ca. 14.5 ka, and three increases of lesser magnitude during the Holocene (Fig. 4). The onset of the pollen record and the largest D/SS peak are probably linked to the formation of the lake. D/SS increases occur between ca. 6 and 5 ka, and between ca. 4.5 and 2.5 ka.

4.2 Lake Fúquene (van der Hammen and Hooghiemstra, 2003)

The Fúquene2 record comes from an intra-Andean valley at 2540 m elevation, a position centrally located in the current altitudinal range of Andean forests. The location of Lake Fúquene makes this record highly sensitive to temperature-driven migrations of montane taxa. During glacial times this area was covered by cold Páramo vegetation, and during interglacials sub-Andean forest taxa reached up to ca. 2300 m (Groot et al., 2011). The short distance between sub-Andean forest and the lake explains pollen from sub-Andean taxa also being represented in AP%.

Páramo taxa show high percentages between ca. 30 and 17.5 ka, but also vary at several intervals (Fig. 2). Andean and sub-Andean taxa (AP%) show an overall increase starting around 15.6 ka, with a trough between ca. 13 and 11 ka, and showing some fluctuations during the Holocene. DCA1 follows remarkably well the variability of AP% (Fig. 3), indicating that this ordination axis is probably tracking temperature-driven UFL migrations. Pleistocene downslope migrations of the UFL can be inferred from AP% decreases around 26, 18 and 13 ka (Fig. 3). AP% increases and upslope UFL migrations are observed at ca. 23.3 and 14 ka. D/SS also shows variations that suggest increases in lake levels after at ca. 22, 12, 8 and 3 ka (Fig. 4).

4.3 Lake La Cocha (González-Carranza et al., 2012)

Lake La Cocha sits in a valley at 2780 m elevation on the eastern flank of the Andes. Amazonian moisture causes abundant orographic rains at this site. Centrally located in the current altitudinal range of the Andean forest (2300 to 3650 m elevation), the AP% record also includes taxa from the sub-Andean forest. During the deglaciation, the UFL was below the elevation of the valley and Páramo vegetation surrounded the lake. AP% reflects temperature changes in this record, although inverse hydrological modelling suggests that Holocene vegetation changes at this site are driven both by increased temperature and moisture (Van Boxel et al., 2014).

Andean and sub-Andean taxa (AP%) in this record increase consistently while Páramo taxa decrease at the Pleistocene-Holocene transition (Fig. 2). Short but clear increases of AP% are detected around 11.5, 9.5, 8 ka. The trend of DCA1 z-scores closely follows AP% (Fig. 3). AP% variability increases during the Holocene and displays a shift around 6 ka. Two increases in D/SS suggest lake level increases between ca. 11 and 6 ka, and between ca. 4 and 2 ka, interrupted by a decreased lake stand centred ca. 5 ka (Fig. 4).

4.4 Lake Surucucho (Colinvaux et al., 1997)

Lake Surucucho is located at 3180 m elevation. Sub-Andean forests reach up to 2800 m in this part of the Andes, while the subpáramo is found at 3500 m elevation. The Andean forest thus covers a vertical range of approximately 700 m. AP% values include Andean taxa at this site and reflect UFL shifts.

Puna and subpuna taxa dominate the pollen record during the late Pleistocene (Fig. 2). Andean forest taxa increase gradually from ca. 12 ka and remain relatively abundant during the Holocene, despite the persistent abundance of Puna and subpuna taxa. DCA1 z-scores and AP% follow a similar trend indicating that temperature is their common driver (Fig. 3). AP% decreases before 18 ka and increases again around 14.5 ka. At ca. 11.3 ka we observe a two-fold increase in AP% and a shift in DCA1 z-scores. D/SS is relatively high during the late Pleistocene with a peak at ca. 17 ka. D/SS decrease after ca. 10 ka and are low throughout the Holocene (Fig. 4).

4.5 Lake Chochos (Bush et al., 2005)

Lake Chochos is located at 3285 m elevation and sits on the eastern flank of the Andes. The record is centrally located in the altitudinal range of UFL glacial-interglacial migrations. AP% includes Andean taxa and is expected to reflect temperature-driven UFL shifts at this site.

Percentages of Andean forest taxa (AP%) are high at the end of the Pleistocene and gradually decrease between ca. 17 and 12 ka (Fig. 2). Andean taxa show some fluctuations during this interval, while Puna and subpuna taxa increase. Between ca. 12 and 10 ka, Andean taxa dominate the record again and Puna and subpuna taxa show relatively low proportions. AP% and DCA1 z-scores show different trends, suggesting that different drivers affect these records (Fig. 3). D/SS are high between ca. 14 and 6 ka, with the highest peak centred at ca. 8.2 ka (Fig. 4).

4.6 Lake Pacucha (Valencia et al., 2010)

Lake Pacucha is located at 3095 m elevation in the Peruvian Andes. The vegetation around the lake is strongly influenced by small-scale topography with mesic forests on the windward slopes and xeric forests in the rain shadow areas. The natural UFL lies between 3300-3600 m, where vegetation changes into shrublands of 100 to 200 m vertical extension. Upslope, this shrubby vegetation transitions into herbaceous Puna up to 4300-4500 m. As the site is located ca. 300 m below the UFL, AP% changes are expected to be very sensitive to temperature-driven altitudinal shifts of the UFL. AP% at Lake Pacucha includes Andean taxa.

Puna and subpuna taxa dominate until ca. 15.6 ka. Andean forest taxa then show a three-fold increase and exceed Puna and subpuna taxa proportions by at least 10%, displaying a peak centred around 15 ka (Fig. 2). Puna and subpuna taxa increase again at ca. 13 ka, while the percentages of Andean forest taxa decrease approximately two-fold. Andean forest taxa percentages recover after ca. 11.5 ka. During the Holocene, both Andean forest and Puna taxa vary and appear to follow the same trend. AP% varies independently from DCA1 z-scores, indicating little correlation between the two markers (Fig. 3). D/SS is high and shows several fluctuations until ca. 11.9 ka, with minima around 18 and 16.5 ka.

4.7 Lake Consuelo (Urrego et al., 2010) Neotoma ID-numbers 17995, 18051.

Lake Consuelo is located at 1360 m on the eastern flank of the Andes. Amazonian moisture causes significant orographic rains at this site, covering the lake in semi-permanent ground-level clouds. Located in the lower part of the current altitudinal range of sub-Andean forest, the AP% record is mainly composed of sub-Andean taxa. Lowland taxa were grouped for Lake Consuelo, but showed less variation than sub-Andean taxa. The vertical distance from Lake Consuelo to the UFL is large, and even during glacial times the lake remained surrounded by cool Andean forests. Changes in AP% are expected to reflect temperature-driven shifts of sub-Andean forests.

Sub-Andean forest taxa dominate the record and reach up to 80% (Fig. 2). Despite its mid-elevation location, the record shows over 30% of the subpuna vegetation during the Pleistocene. The trends of DCA1 z-scores and AP% are similar, but the signals seem more consistent during the Holocene (Fig. 3). D/SS are low between ca. 30 and 10 ka, and show a series of early- Holocene peaks centred around 8 ka (Fig. 4). During the early and late Holocene D/SS are primary low.

4.8 Lake Titicaca (Paduano et al., 2003; Hanselman et al., 2011)

Lake Titicaca is located at 3810 m elevation; the highest site in our transect study. Today

the lake is surrounded by Puna vegetation, and Andean forests occur below 3200 m. Glaciers must have reached the lake basin during glacial times and vegetation comparable to the modern Puna brava (4500-5300 m) probably surrounded the lake. AP% includes Andean taxa and is expected to reflect altitudinal shifts of the UFL. However, the significant distance between the UFL and the lake (between ca. 600 and 1500 m) potentially causes two sources of bias in the AP% values: (1) registered changes in AP% may not be sensitive to minor changes in UFL position and (2) AP% increases may lead the real migration of the UFL due to upslope aeolian pollen transport (Jansen et al., 2013).

Two pollen records are available from Lake Titicaca, and in both Puna taxa dominate the pollen spectra (Fig. 2). Andean forest taxa account for less than 10% of the pollen sum, and reflect the downslope location of the UFL. Puna taxa fluctuate during the Pleistocene, and decrease between ca. 17.8 and 13.8 ka. DCA1 z-scores and AP% fluctuate differently during the Pleistocene, but are consistent during the Holocene (Fig. 3). The core from the centre of the lake did not record aquatic vegetation and D/SS could only be calculated for the record collected closer to the shore. However, given the lake's size and depth, the abundance of shoreline and shallow aquatics is still very low. D/SS is mostly driven by deep-water indicators and is therefore not comparable with the other records (Fig. 4).

5. Discussion

5.1 Extracting climatic information from pollen records

Our comparison of AP% and DCA1 z-scores to extract climate change information from pollen records allows us to highlight differences between the two approaches. On the one hand, ordination analyses like DCA attempt to find the clearest relationships within the pollen dataset, both between pollen taxa and between time slices. The strongest source of variability in one dataset may be precipitation while it may be temperature in another. As a result, ordination scores are not always comparable between sites even after standardization. Relationships between pollen taxa may be due to ecological affinities, and in this sense, this step of the ordination analysis is somewhat equivalent to the taxa grouping done for AP%. However, ordination analyses do not involve *a priori* information (i.e. ecological knowledge) and are only driven by the main sources of variability within the pollen dataset. This is why ordination analyses have been argued to have an advantage over AP%: because each pollen taxon is free to be correlated with any other taxon (Urrego et al., 2005; Colinvaux et al., 1996; Bush et al., 2004). A taxon that today would be grouped as Andean is free to have more affinity with lowland

taxa in the past. It is difficult to allow for this flexibility with AP%, which uses modern ecology to group fossil taxa. On the other hand, ordination analyses produce results that require ecological knowledge for interpretation. The ordination results consist of axis scores for pollen taxa and for time slices that are non-dimensional, lack direction, and can be rotated as desired (Hill and Gauch, 1980). Additionally, information extracted from the ordination axes can only be used in relative terms. As a result, *a posteriori* ecological knowledge of the taxa with the highest loadings is necessary to interpret the main sources of variability within the pollen dataset. Ordination-based interpretation of pollen records may be more appropriate for non-analogue species re-assortments, but still requires knowledge on modern species affinities to extract climate or environmental change information from ordination results.

Using *a priori* ecological knowledge to calculate AP% has been criticized due to potential subjectivity involved in the classification of pollen taxa (Colinvaux et al., 1997). This potential subjectivity relates to the fact that boundaries between vegetation formations are rarely clear cut, hence ecological grouping of transitional or wide-raging taxa is left to the palynologist's discretion. AP% has also been criticised because of the underlying assumption that species respond to change as an assemblage rather than individualistically (Urrego et al., 2010). The record from Lake La Cocha reveals individualistic changes in pollen abundance (González-Carranza et al., 2012), but also clear variations in AP% that may respond to shifting Andean and sub-Andean associations. The record of Lake La Cocha is therefore a good example of how ecological grouping associated with AP% allows for individualist migrations within groups.

The main advantage AP% has over ordination scores is that AP% gives a direction to the observed change from the start. AP% can be translated into temperature-driven UFL migrations (Hooghiemstra et al., 2012) and is comparable between sites. Such site-to-site comparisons of ordination scores are not possible because DCA results are driven by the main source of variability within each site, and this may differ from one site to the other. AP% is also particularly sensitive in high to mid-elevation sites. For instance in Fúquene and Pacucha, AP% is relatively high during the Holocene compared to the Pleistocene (Fig. 3) indicating the signal of post-glacial warming. The sensitivity of AP% can be low however where forest composition remains within one ecological group. In Lake Consuelo AP% remains high during the last glacial and interglacial periods, indicating that the area had a relatively stable forest cover. Despite differences in site sensitivity, AP% changes are comparable between sites.

We also calculated RoC (Urrego et al., 2009) and D/SS ratios to explore their sensitivity to environmental change. RoC values appear to be sensitive to changes in

sedimentation rate, while showing little difference when calculated based on DCA results vs. raw pollen percentages. As an example of this sensitivity we show RoC calculated for the La Cocha record (Fig. S1). We refrain from using RoC in this paper as age uncertainties may be inflated when pollen records of varying quality are compared. One way to circumvent RoC dependency on age and sedimentation uncertainties is to preserve the ecological dissimilarity distances calculated between pollen assemblages as a measure of pollen taxa turnover (for an example see Urrego et al. (2013)).

Another climate change indicator calculated here from pollen records is the D/SS ratio. Assuming that the lakes have minimal losses by underground leaks or outflow, D/SS values potentially indicate lake level changes due to fluctuations in precipitation and evaporation. Increases in D/SS are associated with high abundance of deep-aquatic taxa and likely indicate high lake-level stands. Low D/SS indicates relatively high abundance of aquatic vegetation from shallow waters and reduced water bodies. A potential bias for D/SS is that some taxa included in the 'aquatic pollen sum' have different growth forms. For instance, *Isöetes* is an aquatic fern growing up to 6-m water depth in lakes and is indicative of relatively deep-water conditions. However, in fluvial and fluvio-lacustrine environments *Isöetes* species may also occur on sand banks (Torres et al., 2005). The D/SS ratio is based on relative abundances and is calculated in the same way for all sites. Therefore, calculating D/SS makes differences in pollen/spore production a systematic bias, and allows comparisons among sites and samples within one record. Additionally, the sensitivity of D/SS may depend on water depth. In Lake Titicaca for instance where water depth is more than 200 m, the D/SS ratio is uninformative because no aquatic taxa were recorded (Fig. 4).

5.2 Temperature and moisture availability during the Pleistocene to Holocene transition in the tropical Andes

The eight pollen records from the tropical Andes consistently record Pleistocene altitudinal migrations of Andean and sub-Andean forests linked to glacial cooling. Páramo and subpáramo, or Puna and subpuna vegetation characterize the Pleistocene, while the Holocene is characterised by sub-Andean and Andean forest (Fig. 2). Such forest migrations and inferred temperature change are consistent with other pollen records from the region (e.g. Hansen et al. (2003)), tropical air temperatures changes derived from Andean ice-core isotopic signals (Thompson, 2005), dating of Andean moraines (Smith et al., 2008; van der Hammen et al., 1980/1981), high-elevation Andean lake $\delta^{18}O$ records (Baker et al., 2001; Seltzer et al., 2000), and $\delta^{18}O$ from Andean speleothems (Cheng et al., 2013). SST reconstructions from the western tropical Atlantic

similarly document large fluctuations between the Late Pleistocene and Holocene (Rühlemann et al., 1999), but their magnitude is believed to be less than air-temperature changes recorded by the vegetation and other terrestrial markers.

The pollen records show an overall warming trend during the Pleistocene-Holocene transition, but the onset of post-glacial warming differs in timing among records. Taking the Fúquene record as an example for the northern Andean sites, the first post-glacial warming occurred around 15.6 ka (Fig. 2), but is interrupted by a cooling period between ca. 13 and 11 ka. In Lake Surucucho, the record of Andean forest taxa suggests a steady increase in air temperatures starting around 13 ka. On the other hand, the record of Lake Pacucha in the southern Andes shows a clear trend towards warming starting around 15.6 ka, with a relatively short-lived cooling between ca. 13 and 11.5 ka, followed by another warming. These differences in the onset of post-glacial warming in the Andes are consistent with reconstructions of snowline depressions starting ca. 21 ka in the Peruvian Andes (Smith et al., 2005), the onset of SST warming in the tropical Atlantic ca. 17 ka (Rühlemann et al., 1999), and shifts in stable oxygen isotopes from the Sajama ice cap at ca. 15.5 ka (Thompson et al., 1998).

Changes in D/SS in the selected sites suggest that Pleistocene moisture availability differed from that of the Holocene. D/SS in Northern Andean sites (i.e., Llano Grande, Fúquene, and La Cocha) may indicate increasing lake levels during the Pleistocene-Holocene transition (Fig. 4). Another increase in lake levels is recorded at Fúquene and La Cocha around 8 ka, but not in Llano Grande. Central and Southern sites (i.e. Surucucho, Pacucha, Titicaca and the onset of the pollen record in Lake Chochos) indicate large water bodies and probably high moisture availability through the Pleistocene-Holocene transition and up to 8 ka. D/SS in Lake Consuelo follows a different trend to that observed in other central and southern Andean sites during the late Pleistocene. These differences may be due to the buffering effect of semi-permanent ground-level cloud cover during the last glacial (Urrego et al., 2010). D/SS in lakes Consuelo and Chochos suggest high lake-level stands between ca. 10 and 6 ka and peaking around 8 ka (Fig. 4), analogous to D/SS increases observed in Northern Andean sites. Moisture in Northern Andean sites is mostly linked to the ITCZ, while southern sites are mostly influenced by precipitation from the SASM (Table 1). Overall, these data suggest a north-south difference in lake levels and moisture availability during the Pleistocene-Holocene transition that are consistent with glacial-interglacial atmospheric reorganisations of the ITCZ (Haug et al., 2001) and the SASM (Cruz et al., 2006).

5.3 The signature of millennial-scale climate changes in the tropical Andes

The signature of millennial-scale climate variability is discernible in most pollen records used for our analysis (Fig. 3). AP% decreases in Fúquene, Surucucho and Pacucha approximately coincide with the timing of HS1 (18-15.6 ka, Sánchez Goñi and Harrison (2010). In Lake Titicaca AP% increases during HS1, but the direction of this change is comparable with the change in other records because of the altitudinal location of the site, i.e. above treeline. HS2 (26.5-24.3 ka, Sánchez Goñi and Harrison, 2010) is also insinuated in the low-resolution record from Fúquene by a slight decrease in AP%. In Llano Grande, two AP% decreases observed during the Pleistocene-Holocene transition are roughly consistent with the timing of the Younger Dryas (YD, 12.9-11.6 ka, (Rasmussen et al., 2006; Mangerud et al., 1974). Decreases in AP% during the YD are also apparent in Fúquene, Surucucho, Chochos, and Pacucha. The AP% fluctuations observed during North-Atlantic millennial-scale cooling events are best explained by downslope migrations of Andean vegetation and the UFL linked to air temperature cooling in the tropical Andes.

The AP% records from Lake La Cocha and Consuelo appear to be less sensitive to millennial-scale air temperature cooling recorded in the other sites. In Consuelo in particular the signature of post-glacial warming is marked in the DCA1 z-scores but not in AP% (Fig. 3). DCA1 z-cores in Consuelo only show a few millennial-scale variations that seem unrelated to North-Atlantic cooling events. AP% in Consuelo remains largely unchanged and indicates continuous Andean and sub-Andean forest cover at this site throughout the record (Urrego et al., 2010). The low sensitivity of AP% in Consuelo may also be related to the distance between the site and the UFL as well as the buffering effect of ground-level cloud cover. In La Cocha, UFL sits closer to the site but millennial-scale and centennial-scale climate variability seem to be superimposed in the record (González-Carranza et al., 2012). La Cocha is also a site constantly influenced by ground-level cloud, which may buffer the effect of air temperature cooling on the vegetation.

The signature of GI warming events is best shown for GI1, while the signals of GI2, GI3 and GI4 are hardly recorded (Fig. 3). GI1 (14.6-12.7 ka, Wolff et al., 2010) is suggested by AP% increases in Llano Grande, Fúquene, Surucucho, Chochos and Pacucha. These AP% increases seem more conspicuous and of longer duration in Fúquene and Pacucha. Shifts in DCA1 z-scores are also apparent around the onset of GI1 in Chochos and Consuelo. In the record from Lake Titicaca, the signal of GI1 is either weak or not captured due to the elevation of the site. The onset of the records from Llano Grande and La Cocha probably indicates the formation of these two lakes during GI1 and may be due to increased regional moisture and/or glacial retreats. Differences between

612 the signal of GI1 and other warming events may be related to the duration of this
613 warming event in Greenland compared with other GI. Lasting 1900 years (Wolff et al.,
614 2010), GI1 is more likely to be captured in records with the resolution available for this
615 regional comparison (Table 1). Overall, GI1 potentially coincides with upslope UFL
616 migration and regional warming in the tropical Andes, as well as the formation of some
617 Andean lakes.
618 One important question is whether the signature of millennial-scale climate
619 variability is consistent in the northern and southern tropical Andes. The signature of HS
620 and YD are generally recorded as downslope UFL migrations and air temperature cooling
621 in our transect. Based on the longer records, we also observe a temporal consistency
622 between the signals of different HS. HS1 and HS2 are both linked to AP% decreases and
623 cooling in Fúquene, although the magnitude of change differs. The GI1 signal is overall
624 comparable between northern and southern records and indicates upslope UFL migrations
625 in the tropical Andes. These trends are spatially consistent between northern and southern
626 sites, and imply a common forcing. Air temperature cooling during HS and YD could
627 potentially be linked to cold front advection from the Northern hemisphere reaching as
628 far as 13ºS (Pacucha) or 16ºS if we take the record from Titicaca into account. Cold
629 advection both from the northern and southern hemisphere are common in the tropical
630 Andes and can produce freezing conditions down to 2500 m elevation (Gan and Rao,
631 1994). The air temperature cooling recorded by the Andean vegetation during YD and
632 HS1 could be explained by increased intensity or frequency of northern hemisphere cold
633 advection. On the other hand, upslope UFL migrations and air temperature warming
634 during GI1 could be related to reduced intensity or frequency of northern hemisphere
635 cold advection.
636 To address the consistency of air temperature change recorded by the Andean
637 vegetation with changes recorded by the ocean and the cryosphere, we compare the
638 pollen records from Fúquene and Pacucha with SST reconstructions from the Guyana
639 Basin and the isotopic record from the Sajama ice cap (Fig. 5). Fúquene and Pacucha are
640 used for this comparison as a northern and a southern Andean site, respectively. We also
641 plot the NGRIP and EPICA isotope records in an attempt to assess the relative
642 importance of northern-hemisphere versus southern-hemisphere forcing. Air temperature
643 fluctuations recorded by the Andean vegetation both in the northern and southern Andes
644 are consistent with changes in tropical Atlantic SST (Rama-Corredor et al., 2015) and the
645 isotopic record from the Sajama ice cap (Thompson et al., 1998), especially during HS1,
646 GI1 and YD (Fig. 5), When compared with the long-term variability within each record,
647 the amplitude of change recorded by the Andean vegetation during GI1 and YD seems

comparable to that of the Sajama ice core record. The vegetation records and the isotopic signal of the Sajama ice core are comparable despite differences in moisture sources, reiterating that together these changes are best explained by fluctuations in air temperature. The SST record from the tropical Atlantic suggests reduced amplitude of temperature changes during the same period compared to the Andean vegetation and the ice core record. This comparison suggests a potential difference between the magnitude of temperature change in the ocean and the atmosphere that could relate to the thermal inertia of the ocean. Additionally, the climatic trends observed in the Andean records are comparable to the Greenland ice core record (NGRIPmembers, 2004), and show fewer similarities with Antarctica (EPICA, 2006). The observed similarities point to northern-hemisphere climate variability forcing UFL migrations and air temperature cooling in the northern and southern tropical Andes during HS and YD.

Millennial-scale vegetation changes in the tropical Andes show great variability, and appear to be asynchronous to those of tropical Atlantic SST and the isotopic signal of Andean ice core records (Fig. 5). Vascular plant biomarkers preserved in the Cariaco Basin have suggested that tropical vegetation lagged climate change by several decades (Hughen et al., 2004). A similar time lag between the response of vegetation and marine markers in northeastern South America is estimated to be 1000 to 2000 years during HS (Jennerjahn et al., 2004). Our explorations with regard to the asynchronicity of these signals remain within the constraints of available dating and sampling resolution. However, our results suggest that vegetation responses to millennial-scale climate variability are overall very rapid.

6. Conclusions

Records of past vegetation change in the tropical Andes showed that altitudinal migrations of the vegetation are best explained by millennial-scale cooling and warming of air temperatures linked to northern-hemisphere forcing. Taking into account differences in the sensitivity of individual sites, the signature of HS is overall consistent among northern and southern Andean records and indicates downslope shifts of the UFL and cooling. The air temperature cooling needed to produce such migrations could potentially have resulted from increased intensity and duration of cold advection from the northern hemisphere. GI1 potentially coincides with upslope UFL migration and regional warming in the tropical Andes, as well as the formation of some Andean lakes. The air temperature change recorded by the Andean vegetation was consistent with millennial-scale cryosphere and ocean temperature changes, but suggests a potential difference between the magnitude of temperature change in the ocean and the atmosphere. Our

analysis also suggests a north-south difference in the moisture availability during the Pleistocene-Holocene transition that can potentially be related to reorganisations of the ITCZ and the SASM.

We showed that AP% and DCA scores, two approaches to extract environmental variability from pollen records, are complementary rather than divergent. Transforming raw pollen counts into percentages of ecologically meaningful groups (e.g. AP%) or into ordination values results in records that are seldom driven by similar factors. The two approaches rely on a reasonable understanding of ecological affinities and knowledge of the regional vegetation. This information is used *a priori* for AP% and *a posteriori* for ordination scores. AP% and DCA axis scores remain as vegetation markers and are not independent records of environmental change. Such records are still needed for most of the studied sequences. Along with the development of pollen records, independent markers of temperature or precipitation (i.e. biochemical or isotopic markers) are needed in the American tropics (Urrego et al., 2014), and future work should preferably generate combinations of proxies to disentangle differences between the magnitude of atmospheric and oceanic change. Integrated multi-tracer approaches will help minimize chronological uncertainty and may shed light on the underlying forcing of these rapid shifts in the climate system.

7. Acknowledgements

This paper is a result of the project 'Latin American Abrupt Climate Changes and Environmental Responses' (LaACER) funded by PAGES and INQUA. B.M. thanks CSIC-Ramón and Cajal post-doctoral program RYC-2013-14073.

The plot data of this manuscript is freely available from: ***

8. References

Arz, H. W., Pätzold, J., and Wefer, G.: Correlated millennial-scale changes in surface hydrography andd terrigenous sediment yield inferred from the last-glacial marine deposits off Northeastern Brazil, Quaternary Research, 50, 157-166, 1998.

Baker, P. A., Rigsby, C. A., Seltzer, G. O., Fritz, S. C., Lowenstein, T. K., Bacher, N. P., and Veliz, C.: Tropical climate changes at millennial and orbital timescales on the Bolivian Altiplano., Nature, 409, 698-701, 2001.

Bakker, J., Moscol, M., and Hooghiemstra, H.: Holocene environmental change at the upper forest line in northern Ecuador, The Holocene, 18, 877-893, 2008.

719 Birks, H. J. B., and Birks, H. H.: Quaternary Palaeoecology, University Park Press,
720 Baltimore, 1980.

721 Bogotá, R. G., Groot, M. H. M., Hooghiemstra, H., Lourens, L. J., Linden, M. V. d., and
722 Berrio, J. C.: Rapid climate change from north Andean Lake Fúquene pollen records
723 driven by obliquity: implications for a basin-wide biostratigraphic zonation for the last
724 284 ka, Quaternary Science Reviews, 30, 3321-3337, 10.1016/j.quascirev.2011.08.003,
725 2011.

726 Broccoli, A. J., Dahl, K. A., and Stouffer, R. J.: Response of the ITCZ to Northern
727 Hemisphere cooling, Geophysical Research Letters, 33, L01702, doi:
728 10.1029/2005GL024546, 2006.

729 Bush, M. B., Silman, M. R., and Urrego, D. H.: 48,000 years of climate and forest change
730 in a biodiversity hot spot, Science, 303, 827-829, doi:10.1126/science.1090795, 2004.

731 Bush, M. B., Hansen, B. C. S., Rodbell, D. T., Seltzer, G. O., Young, K. R., León, B.,
732 Abbott, M. B., Silman, M. R., and Gosling, W. D.: A 17 000-year history of Andean
733 climate and vegetation change from Laguna de Chochos, Peru, Journal of Quaternary
734 Science, 20, 703-714, 2005.

735 Cheng, H., Sinha, A., Cruz, F. W., Wang, X., Edwards, R. L., d'Horta, F. M., Ribas, C.
736 C., Vuille, M., Stott, L. D., and Auler, A. S.: Climate change patterns in Amazonia and
737 biodiversity, Nature communications, 4, 1-6, DOI: 10.1038/ncomms2415, 2013.

738 Chiang, J. C., and Bitz, C. M.: Influence of high latitude ice cover on the marine
739 Intertropical Convergence Zone, Climate Dynamics, 25, 477-496, 2005.

740 Colinvaux, P. A., De Oliveira, P. E., Moreno, J. E., Miller, M. C., and Bush, M. B.: A
741 long pollen record from lowland Amazonia: Forest and cooling in glacial times., Science,
742 274, 85-88, 1996.

743 Colinvaux, P. A., Bush, M. B., Steinitz-Kannan, M., and Miller, M. C.: Glacial and
744 postglacial pollen records from the Ecuadorian Andes and Amazon, Quaternary
745 Research, 48, 69-78, 1997.

746 Cruz, F. W., Burns, S. J., Karmann, I., Sharp, W. D., Vuille, M., Cardoso, A. O., Ferrari,
747 J. A., Silva Dias, P. L., and Viana Jr., O.: Insolation-driven changes in atmospheric
748 circulation over the past 116,000 years in subtropical Brazil, Nature, 434, 63-66, 2005.

749 Cruz, F. W., Burns, S. J., Karmann, I., Sharp, W. D., Vuille, M., and Ferrari, J. A.: A
750 stalagmite record of changes in atmospheric circulation and soild processes in the
751 Brazilian subtropics during the Late Pleistocene, Quaternary Science Reviews, 25, 2749-
752 2761, 2006.

753 EPICA: One-to-one coupling of glacial climate variability in Greenland and Antarctica,
754 Nature, 444, 195-198, doi: 10.1038/nature05301, 2006.

755 Escobar, J., Hodell, D. A., Brenner, M., Curtis, J. H., Gilli, A., Mueller, A. D.,
756 Anselmetti, F. S., Ariztegui, D., Grzesik, D. A., and Pérez, L.: A~ 43-ka record of
757 paleoenvironmental change in the Central American lowlands inferred from stable
758 isotopes of lacustrine ostracods, Quaternary Science Reviews, 37, 92-104, 2012.

759 Fritz, S. C., Baker, P. A., Ekdahl, E., Seltzer, G. O., and Stevens, L. R.: Millennial-scale
760 climate variability during the Last Glacial period in the tropical Andes, Quaternary
761 Science Reviews, 29, 1017-1024, 2010.

762 Fu, R., Dickinson, R. E., Chen, M., and Wang, H.: How do tropical sea surface
763 temperatures influence the seasonal distribution of precipitation in the equatorial
764 Amazon?, Journal of Climate, 14, 4003-4026, 2001.

765 Gan, M. A., and Rao, V. B.: The influence of the Andes Cordillera on transient
766 disturbances, Monthly Weather Review, 122, 1141-1157, 1994.

767 Garreaud, R., and Wallace, J. M.: Summertime incursions of midlatitude air into
768 subtropical and tropical South America, Monthly Weather Review, 126, 2713-2733,
769 1998.

770 Garreaud, R. D.: Cold air incursions over subtropical South America: Mean structure and
771 dynamics, Monthly Weather Review, 128, 2544-2559, 2000.

772 Garreaud, R. D., Vuille, M., Compagnucci, R., and Marengo, J.: Present-day South
773 American climate, Palaeogeography, Palaeoclimatology, Palaeoecology, 281, 180-195,
774 doi:10.1016/j.palaeo.2007.10.032, 2009.

775 González-Carranza, Z., Hooghiemstra, H., and Vélez, M. I.: Major altitudinal shifts in
776 Andean vegetation on the Amazonian flank show temporary loss of biota in the
777 Holocene, The Holocene, 22, 1227-1241, 10.1177/0959683612451183, 2012.

778 Graham, A.: The Andes: a geological overview from a biological perspective, Ann.
779 Missouri. Bot. Gard., 96, 371-385, 2009.

780 Groot, M., Bogotá, R., Lourens, L., Hooghiemstra, H., Vriend, M., Berrio, J., Tuenter, E.,
781 Van der Plicht, J., Van Geel, B., and Ziegler, M.: Ultra-high resolution pollen record
782 from the northern Andes reveals rapid shifts in montane climates within the last two
783 glacial cycles, Climate of the Past, 7, 299-316, doi:10.5194/cp-7-299-2011, 2011.

784 Hanselman, J. A., Bush, M. B., Gosling, W. D., Collins, A., Knox, C., Baker, P. A., and
785 Fritz, S. C.: A 370,000-year record of vegetation and fire history around Lake Titicaca
786 (Bolivia/Peru), Palaeogeography, Palaeoclimatology, Palaeoecology, 305, 201-214, doi:
787 10.1016/j.palaeo.2011.03.002, 2011.

788 Hansen, B. C. S., Rodbell, D. T., Seltzer, G. O., León, B., Young, K. R., and Abbott, M.:
789 Late-glacial and Holocene vegetational history from two sites in the western Cordillera of
790 southwestern Ecuador, Palaeogeography, Palaeoclimatology, Palaeoecology, 194, 79-
791 108, 2003.

792 Harrison, S. P., and Sanchez Goñi, M. F.: Global patterns of vegetation response to
793 millennial-scale variability and rapid climate change during the last glacial period,
794 Quaternary Science Reviews, 29, 2957-2980, 10.1016/j.quascirev.2010.07.016, 2010.

795 Haug, G. H., Hughen, K. A., Sigman, D., Peterson, L. C., and Röhl, U.: Southward
796 Migration of the intertropical convergence zone through the Holocene, Science, 293,
797 1304-1308, 2001.

798 Heinrich, H.: Origin and consequences of cyclic ice rafting in the Northeast Atlantic
799 Ocean during the past 130,000 years, Quaternary Research, 29, 142-152,
800 http://dx.doi.org/10.1016/0033-5894(88)90057-9, 1988.

801 Hemming, S. R.: Heinrich events: Massive late Pleistocene detritus layers of the North
802 Atlantic and their global climate imprint, Reviews of Geophysics, 42, RG1005, DOI:
803 10.1029/2003RG000128, 2004.

804 Hessler, I., Dupont, L., Bonnefille, R., Behling, H., González, C., Helmens, K. F.,
805 Hooghiemstra, H., Lebamba, J., Ledru, M.-P., LÉzine, A.-M., Maley, J., Marret, F., and
806 Vincens, A.: Millennial-scale changes in vegetation records from tropical Africa and
807 South America during the last glacial, Quaternary Science Reviews, 29, 2882-2899, doi:
808 10.1016/j.quascirev.2009.11.029, 2010.

809 Hill, M. O., and Gauch, H. G.: Detrended Correspondence Analysis: an improved
810 ordination technique, Vegetatio, 42, 47-58, 1980.

811 Hooghiemstra, H.: Vegetational and climatic history of the high plain of Bogota,
812 Colombia: A continuous record of the last 3.5 million Years, Gantner Verlag, Vaduz, 368
813 pp., 1984.

814 Hooghiemstra, H., and van der Hammen, T.: Quaternary ice-age in the Colombian
815 Andes: developing an understanding of our legacy, Philosophical Transactions of the
816 Royal Society of London 359, 173-181, 2004.

817 Hooghiemstra, H., Berrio, J. C., Groot, M. H., Bogotá-A, R. G., Olivera, M. M., and
818 González-Carranza, Z.: The dynamic history of the upper forest line ecotone in the
819 northern Andes, in: Ecotones Between Forest and Grassland, Springer, New York,
820 Heidelberg, Dordrecht, London, 229-246, 2012.

821 Hooghiemstra, H., Berrio, J.C., Groot, M.H.M., Bogotá-A, R.G., Moscol-Olivera, M.,
822 González-Carranza, Z.: The dynamic history of the upper forest line ecotone in the
823 northern Andes, in: Ecotones between forest and grassland, edited by: Randall, R. W.,
824 Springer Science+Business Media, New York, Heidelberg, Dordrecht, London, 229-246,
825 2012.

826 Hughen, K. A., Overpeck, J. T., Peterson, L. C., and Trumbore, S.: Rapid climate
827 changes in the tropical Atlantic region during the last deglaciation, Nature, 380, 51-54,
828 1996.

829 Hughen, K. A., Eglinton, T. I., Xu, L., and Makou, M.: Abrupt Tropical Vegetation
830 Response to Rapid Climate Changes, Science, 304, 1955-1959, 2004.

831 Jansen, B., de Boer, E. J., Cleef, A. M., Hooghiemstra, H., Moscol-Olivera, M.,
832 Tonneijck, F. H., and Verstraten, J. M.: Reconstruction of late Holocene forest dynamics
833 in northern Ecuador from biomarkers and pollen in soil cores, Palaeogeography,
834 Palaeoclimatology, Palaeoecology, 386, 607-619, 2013.

835 Jennerjahn, T. C., Ittekkot, V., Arz, H. W., Behling, H., Pätzold, J., and Wefer, G.:
836 Asynchronous Terrestrial and Marine Signals of Climate Change During Heinrich
837 Events, Science, 306, 2236-2239, 10.1126/science.1102490, 2004.

838 Killeen, T. J., Douglas, M., Consiglio, T., Jørgensen, P. M., and Mejia, J.: Dry spots and
839 wet spots in the Andean hotspot, Journal of Biogeography, 34, 1357-1373, 2007.

840 Körner, C.: The use of 'altitude' in ecological research, Trends in Ecology and Evolution,
841 22, 569-574, DOI: 10.1016/j.tree.2007.09.006, 2007.

842 Lachniet, M. S., Asmerom, Y., Bernal, J. P., Polyak, V. J., and Vazquez-Selem, L.:
843 Orbital pacing and ocean circulation-induced collapses of the Mesoamerican monsoon
844 over the past 22,000 y, Proceedings of the National Academy of Sciences, 110, 9255-
845 9260, 2013.

846 Luteyn, J. L., and Churchill, S. P.: Páramos: a checklist of plant diversity, geographical
847 distribution, and botanical literature, New York Botanical Garden Press New York, 1999.

848 Mangerud, J. A. N., Andersen, S. T., Berglund, B. E., and Donner, J. J.: Quaternary
849 stratigraphy of Norden, a proposal for terminology and classification, Boreas, 3, 109-126,
850 10.1111/j.1502-3885.1974.tb00669.x, 1974.

851 McCune, B., and Grace, J. B.: Analysis of ecological communities, MjM Software
852 Design, Gleneden Beach, Oregon, 300 pp., 2002.

853 Mosblech, N. A. S., Bush, M. B., Gosling, W. D., Hodell, D., Thomas, L., van Calsteren,
854 P., Correa-Metrio, A., Valencia, B. G., Curtis, J., and van Woesik, R.: North Atlantic
855 forcing of Amazonian precipitation during the last ice age, Nature Geoscience, 5, 817-
856 820, 2012.

857 NGRIPmembers: High-resolution record of Northern Hemisphere climate extending into
858 the last interglacial period, Nature, 431, 147-151, 2004.

859 Paduano, G. M., Bush, M. B., Baker, P. A., Fritz, S. C., and Seltzer, G. O.: A vegetation
860 and fire history of Lake Titicaca since the Last Glacial Maximum, Palaeogeography,
861 Palaeoclimatology, Palaeoecology, 194, 259-279, 2003.

862 Peterson, L. C., Haug, G. H., Hughen, K. A., and Röhl, U.: Rapid changes in the
863 Hydrologic cycle of the Tropical Atlantic during the Last Glacial, Science, 290, 1947-
864 1951, 2000.

865 Poveda, G., and Mesa, O. J.: Feedbacks between hydrological processes in tropical South
866 America and large-scale ocean-atmospheric phenomena, Journal of Climate, 10, 2690-
867 2702, 1997.

868 Poveda, G., Waylen, P. R., and Pulwarty, R. S.: Annual and inter-annual variability of the
869 present climate in northern South America and southern Mesoamerica, Palaeogeography,
870 Palaeoclimatology, Palaeoecology, 234, 3-27, 2006.

871 Poveda, G., Álvarez, D. M., and Rueda, Ó. A.: Hydro-climatic variability over the Andes
872 of Colombia associated with ENSO: a review of climatic processes and their impact on
873 one of the Earth's most important biodiversity hotspots, Climate Dynamics, 36, 2233-
874 2249, DOI: 10.1007/s00382-010-0931-y, 2011.

875 Rama-Corredor, O., Martrat, B., Grimalt, J., Lopez-Otalvaro, G. E., Flores, J. A., and
876 Sierro, F. J.: Parallelisms between sea surface temperature changes in the Western
877 Tropical Atlantic (Guiana basin) and high latitude climate signals over the last 140,000
878 years, Climate of the Past, 11, 1297-1311, doi:10.5194/cp-11-1297-2015, 2015.

879 Rasmussen, S. O., Andersen, K. K., Svensson, A. M., Steffensen, J. P., Vinther, B. M.,
880 Clausen, H. B., Siggaard-Andersen, M. L., Johnsen, S. J., Larsen, L. B., Dahl-Jensen, D.,
881 Bigler, M., Röthlisberger, R., Fischer, H., Goto-Azuma, K., Hansson, M. E., and Ruth,
882 U.: A new Greenland ice core chronology for the last glacial termination, Journal of
883 Geophysical Research: Atmospheres, 111, D06102, 10.1029/2005JD006079, 2006.

884 Reese, C. A., and Liu, K.: A modern pollen rain study from the central Andes region of
885 South America, Journal of Biogeography, 32, 709-718, 2005.

886 Reimer, P. J., Bard, E., Bayliss, A., Beck, J. W., Blackwell, P. G., Bronk Ramsey, C.,
887 Buck, C. E., Cheng, H., Edwards, R. L., Friedrich, M., Grootes, P. M., Guilderson, T. P.,
888 Haflidason, H., Hajdas, I., Hatté, C., Heaton, T. J., Hoffmann, D. L., Hogg, A. G.,
889 Hughen, K. A., Kaiser, K. F., Kromer, B., Manning, S. W., Niu, M., Reimer, R. W.,
890 Richards, D. A., Scott, E. M., Southon, J. R., Staff, R. A., Turney, C. S. M., and Plicht, J.
891 v. d.: IntCal13 and Marine13 radiocarbon age calibration curves 0-50,000 years cal BP,
892 Radiocarbon, 55, 1869-1887, 2013.

893 Ruddiman, W. F.: Earth's Climate: past and future, Macmillan, 2001.

894 Rühlemann, C., Mulitza, S., Müller, P. J., Wefer, G., and Zahn, R.: Warming of the
895 tropical Atlantic Ocean and slowdown of thermohaline circulation during the last
896 deglaciation, Nature, 402, 511-514, 1999.

897 Rühlemann, C., Mulitza, S., Lohmann, G., Paul, A., Matthias, P., and Wefer, G.: Abrupt
898 Warming of the Intermediate-Depth Atlantic Ocean in Response to Thermohaline
899 Circulation Slowdown During the last deglaciation, PAGES news, 11, 17-19, 2003.

900 Sánchez Goñi, M. F., and Harrison, S. P.: Millennial-scale climate variability and
901 vegetation changes during the Last Glacial: Concepts and terminology, Quaternary
902 Science Reviews, 29, 2823-2827, 2010.

903 Schmidt, M. W., Spero, H. J., and Lea, D. W.: Links between salinity variation in the
904 Caribbean and North Atlantic thermohaline circulation, Nature, 428, 160-163, 2004.

905 Seltzer, G., Rodbell, D., and Burns, S.: Isotopic evidence for late Quaternary climatic
906 change in tropical South America, Geology, 28, 35-38, 2000.

907 Smith, J. A., Seltzer, G. O., Farber, D. L., Rodbell, D. T., and Finkel, R. C.: Early Local
908 Last Glacial Maximum in the Tropical Andes, Science, 308, 678-681, 2005.

909 Smith, J. A., Mark, B. G., and Rodbell, D. T.: The timing and magnitude of moutain
910 glaciation in the tropical Andes, Journal of Quaternary Science, 23, 609-634,
911 10.1002/jqs.1224, 2008.

912 Thompson, L. G., Davis, M. E., Mosley-Thompson, E., Sowers, T. A., Henderson, K. A.,
913 Zagorodnov, V. S., Lin, P.-N., Mikhalenko, V. N., Campen, R. K., Bolzan, J. F., Cole-
914 Dai, J., and Francou, B.: A 25,000-year tropical climate history from Bolivian ice cores.,
915 Science, 282, 1858-1864, 1998.

916 Thompson, L. G.: Tropical ice core records: evidence for asynchronous glaciations on
917 Milankovitch timescales, Journal of Quaternary Science, 20, 723-733, 2005.

918 Torres, V., Vandenberghe, J., and Hooghiemstra, H.: An environmental reconstruction of
919 the sediment infill of the Bogotá basin (Colombia) during the last 3 million years from
920 abiotic and biotic proxies, Palaeogeography, Palaeoclimatology, Palaeoecology, 226,
921 127-148, 2005.

922 Urrego, D. H., Silman, M. R., and Bush, M. B.: The Last Glacial Maximum: stability and
923 change in a western Amazonian cloud forest, Journal of Quaternary Science, 20, 693-701,
924 2005.

925 Urrego, D. H., Bush, M. B., Silman, M. R., Correa-Metrio, A., Ledru, M.-P., Mayle, F.
926 E., Paduano, G., and Valencia, B. G.: Millennial-scale Ecological Changes in Tropical
927 South America since the Last Glacial Maximum, in: Past climate variability from the Last
928 Glacial Maximum to the Holocene in South America and surrounding regions, edited by:
929 Vimeux, F., Sylvestre, F., and Khodri, M., Developments in Paleoenvironmental
930 Research Series (DPER), Springer, Paris, 283-300, 2009.

931 Urrego, D. H., Bush, M. B., and Silman, M. R.: A long history of cloud and forest
932 migration from Lake Consuelo, Peru, Quaternary Research, 73, 364-373,
933 10.1016/j.yqres.2009.10.005, 2010.

934 Urrego, D. H., Silman, M. R., Correa-Metrio, A., and Bush, M. B.: Pollen-vegetation
935 relationships along steep climatic gradients in western Amazonia, Journal of Vegetation
936 Science, 22, 795-806, 10.1111/j.1654-1103.2011.01289.x, 2011.

937 Urrego, D. H., Bush, M. B., Silman, M. R., Niccum, B. A., De La Rosa, P., McMichael,
938 C., Hagen, S., and Palace, M.: Holocene fires, forest stability and human occupation in
939 southwestern Amazonia, Journal of Biogeography, 40, 521-533, 10.1111/jbi.12016, 2013.

940 Urrego, D. H., Bernal, J. P., Chiessi, C. M., Cruz, F. W., Sanchez Goñi, M. F., Power,
941 M., Hooghiemstra, H., and participants, L.: Millennial-scale climate variability in the
942 American tropics and subtropics, PAGES Mag, 22, 94-95, 2014.

943 Valencia, B. G., Urrego, D. H., Silman, M. R., and Bush, M. B.: From ice age to modern:
944 a record of landscape change in an Andean cloud forest, Journal of Biogeography, 37,
945 1637-1647, 10.1111/j.1365-2699.2010.02318.x, 2010.

946 Van Boxel, J., González-Carranza, Z., Hooghiemstra, H., Bierkens, M., and Vélez, M.:
947 Reconstructing past precipitation from lake levels and inverse modelling for Andean
948 Lake La Cocha, Journal of Paleolimnology, 51, 63-77, 2014.

949 van der Hammen, T., Barelds, J., De Jong, H., and De Veer, A. A.: Glacial sequence and
950 environmental history in the Sierra Nevada del Cocuy (Colombia), Palaeogeography,
951 Palaeoclimatology, Palaeoecology, 32, 247-340, 1980/1981.

952 van der Hammen, T., and Hooghiemstra, H.: Interglacial-glacial Fuquene-3 pollen record
953 from Colombia: an Eemian to Holocene climate record, Global and Planetary Change,
954 36, 181-199, 2003.

955 Velásquez, C. A., and Hooghiemstra, H.: Pollen-based 17-kyr forest dynamics and
956 climate change from the Western Cordillera of Colombia; no-analogue associations and
957 temporarily lost biomes, Review of Palaeobotany and Palynology, 194, 38-49,
958 10.1016/j.revpalbo.2013.03.001, 2013.

959 Vuille, M., and Bradley, R. S.: Mean annual temperature trends and their vertical
960 structure in the tropical Andes, Geophysical Research Letters, 27, 3885-3888, 2000.

961 Vuille, M., Bradley, R. S., and Keimig, F.: Interannual climate variability in the Central
962 Andes and its relation to tropical Pacific and Atlantic forcing., Journal of Geophysical
963 Research, 105, 12447-12460, 2000.

964 Vuille, M., and Werner, M.: Stable isotopes in precipitation recording South American
965 summer monsoon and ENSO variability: observations and model results, Climate
966 Dynamics, 25, 401-413, 2005.

967 Weigend, M.: Observations on the biogeography of the Amotape-Huancabamba Zone in
968 northern Peru, The Botanical Review, 68, 38-54, 10.1663/0006-
969 8101(2002)068[0038:OOTBOT]2.0.CO;2, 2002.

970 Weng, C., Bush, M. B., and Silman, M. R.: An analysis of modern pollen rain on an
971 elevational gradient in southern Peru., Journal of Tropical Ecology, 20, 113-124, 2004.

972 Wolff, E. W., Chappellaz, J., Blunier, T., Rasmussen, S. O., and Svensson, A.:
973 Millennial-scale variability during the last glacial: The ice core record, Quaternary
974 Science Reviews, 29, 2828-2838, 10.1016/j.quascirev.2009.10.013, 2010.

975 Zhou, J., and Lau, K. M.: Does a monsoon climate exist over South America?, Journal of
976 Climate, 11, 1020-1040, 1998.

977 Zhou, J., and Lau, K. M.: Principal modes of interannual and decadal variability of
978 summer rainfall over South America, International Journal of Climatology, 21, 1623-
979 1644, 2001.
980

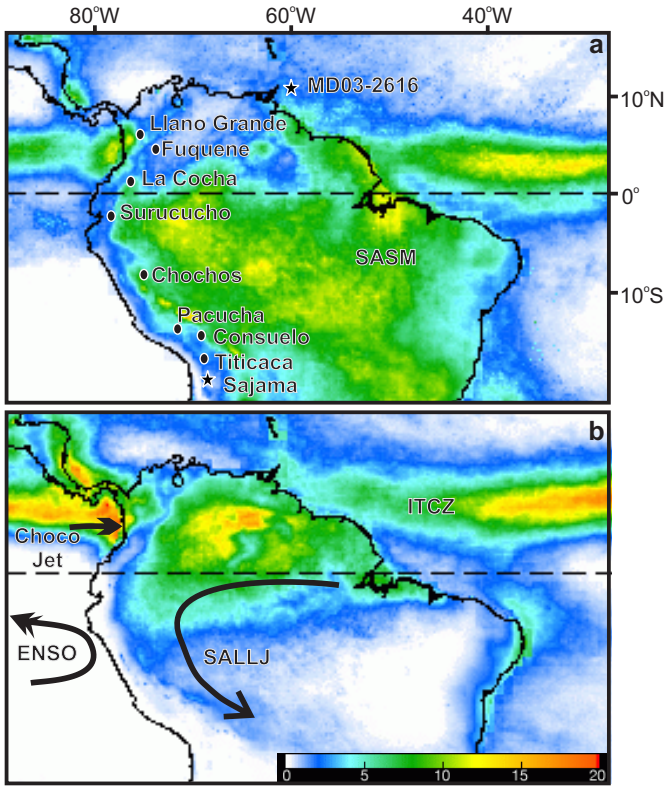

Figure 1. Average daily rainfall rates during the months of January (a) and July (b) from 1998-2007 from the Tropical Rainfall Measuring Mission. Black circles show the locations of pollen records described in Table 1. Stars indicate the location of the sea surface temperature record from the tropical Atlantic (MD03-2616) and the Sajama ice core. The rainfall distribution depicts the average southern and northern positions of the Intertropical Convergence Zone (ITCZ), and the South American Summer Monsoon (SASM). Arrows indicate the approximate location of relevant atmospheric and oceanic systems: South America Low Level Jet (SALLJ), El Niño Southern Oscillation (ENSO) and the Chocó Jet.

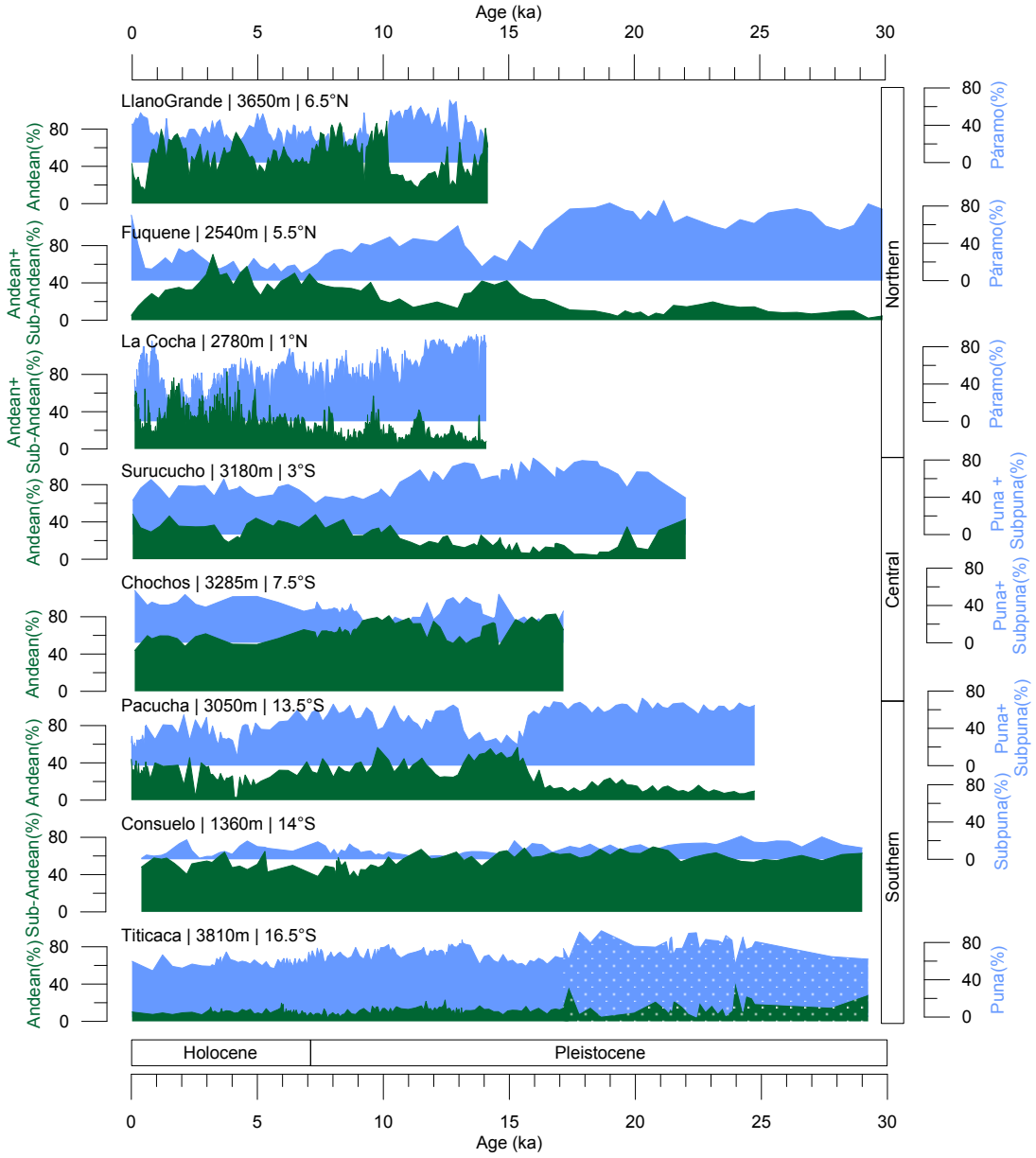

Figure 2. Summary pollen diagrams of selected pollen records from the tropical Andes (Fig. 1, Table 1) plotted on against time in thousands of years (ka). Site name, elevation rounded up to the nearest 5 m, and latitude to the nearest half degree are shown next to each record. Pollen taxa are grouped into Andean and sub-Andean taxa (green) and Páramo, Puna or subpuna taxa (blue). Taxa groupings follow original papers when available. For sites published without ecological groups, taxa have been grouped for the first time. Two pollen records are available from Lake Titicaca, and here they are differentiated with a dotted pattern for the Hanselman et al. (2011) record, and solid pattern for the Paduano et al. (2003) record.

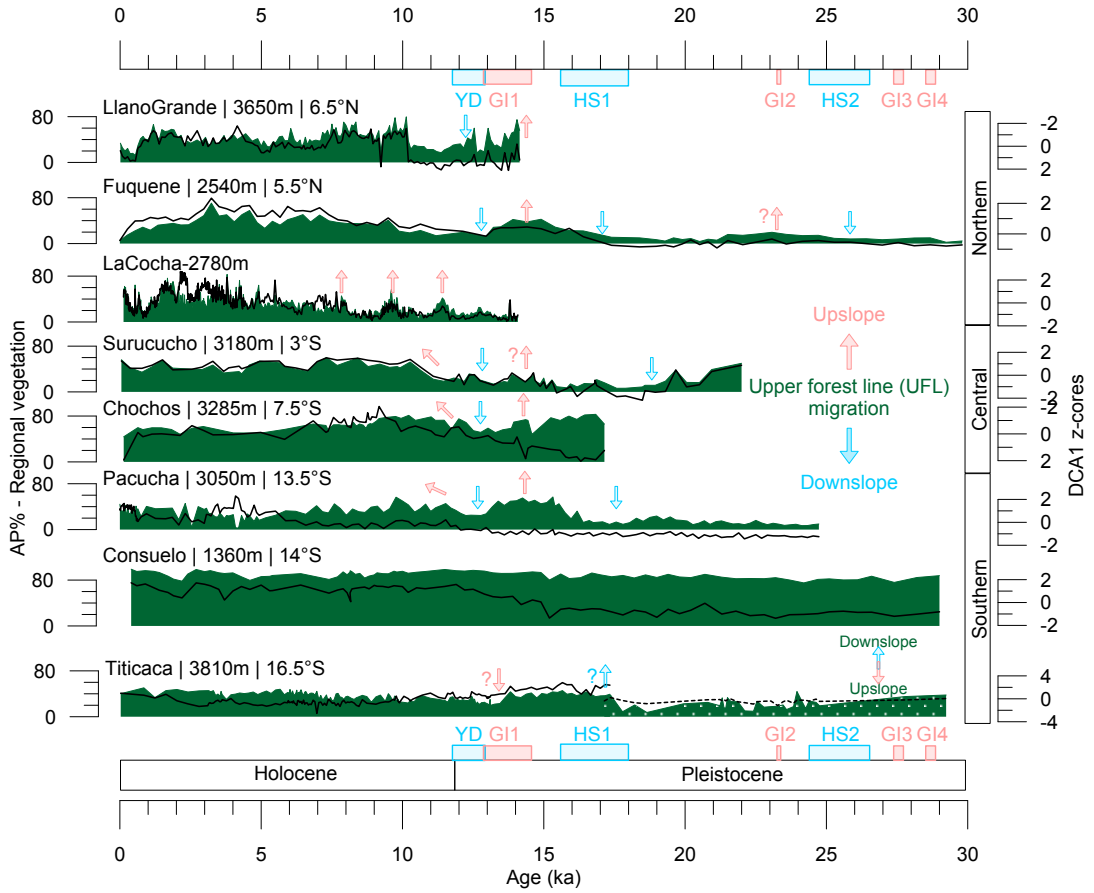

Figure 3. Temporal changes in regional vegetation AP% (green polygons) and DCA1 z-scores (black line) plotted on a linear time scale for selected pollen records from the tropical Andes (Fig. 1, Table 1). Site name, elevation rounded up to the nearest 5 m, and latitude to the nearest half degree are shown next to each record. Two pollen records are available from Lake Titicaca, and here they are differentiated with a dotted pattern for the Hanselman et al. (2011) record, and solid pattern for the Paduano et al. (2003) record. Heinrich stadials (HS) are drawn for reference as defined by Sánchez-Goñi & Harrison (2010). The Younger Dryas (YD) follows the timing of Greenland stadial 1 (Rasmussen et al. 2006) and the chronozone defined by Mangerud et al. (1974). The timing of Greenland interstadials (GI) is based on Wolff et al. (2010).

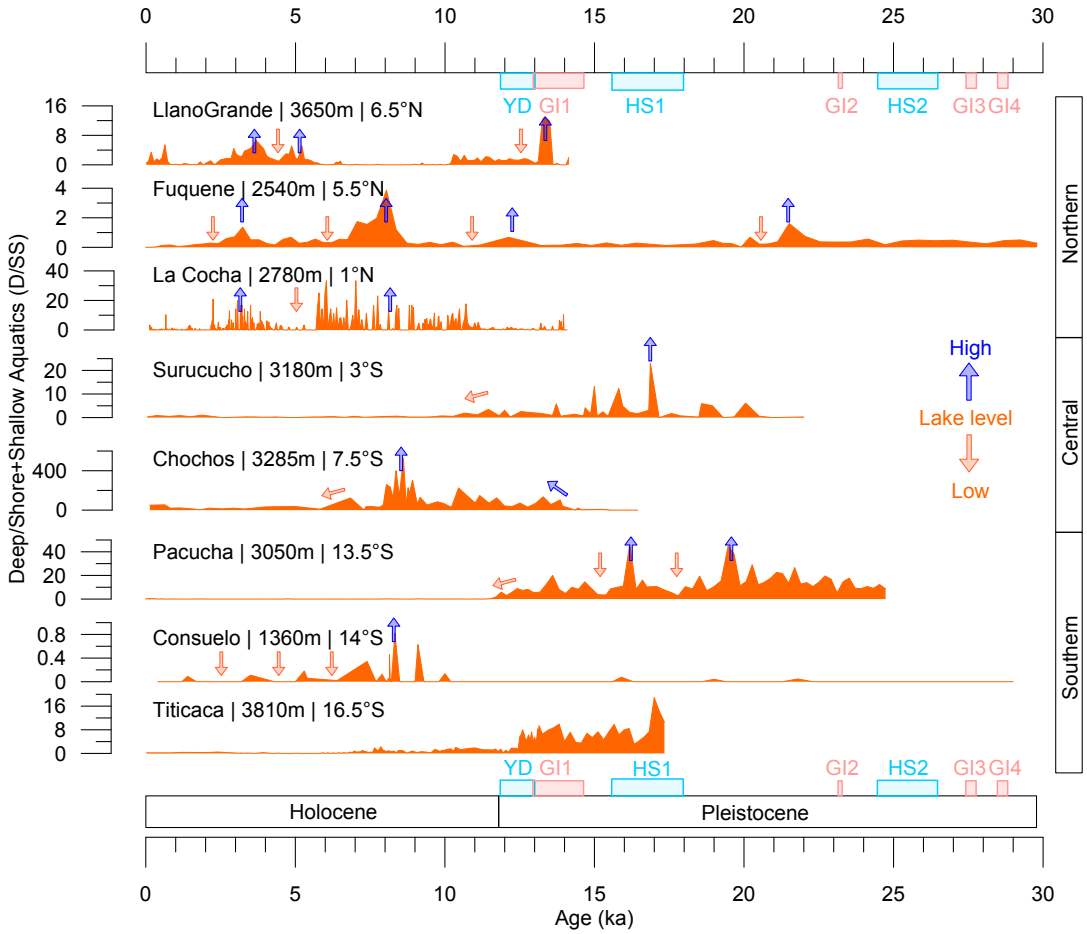

Figure 4. Temporal changes in the ratio of aquatic taxa characteristic of deep water to taxa from shallow water and wet shores (D/SS) for selected sites in the tropical Andes (Fig 1, Table 1). Site name, elevation rounded up to the nearest 5 m, and latitude to the nearest half degree are shown next to each record. Heinrich stadials (HS) are drawn for reference as defined by Sánchez-Goñi & Harrison (2010). The Younger Dryas (YD) follows the timing of Greenland stadial 1 (Rasmussen et al. 2006) and the chronozone defined by Mangerud et al. (1974). The timing of Greenland interstadials (GI) is based on Wolff et al. (2010).

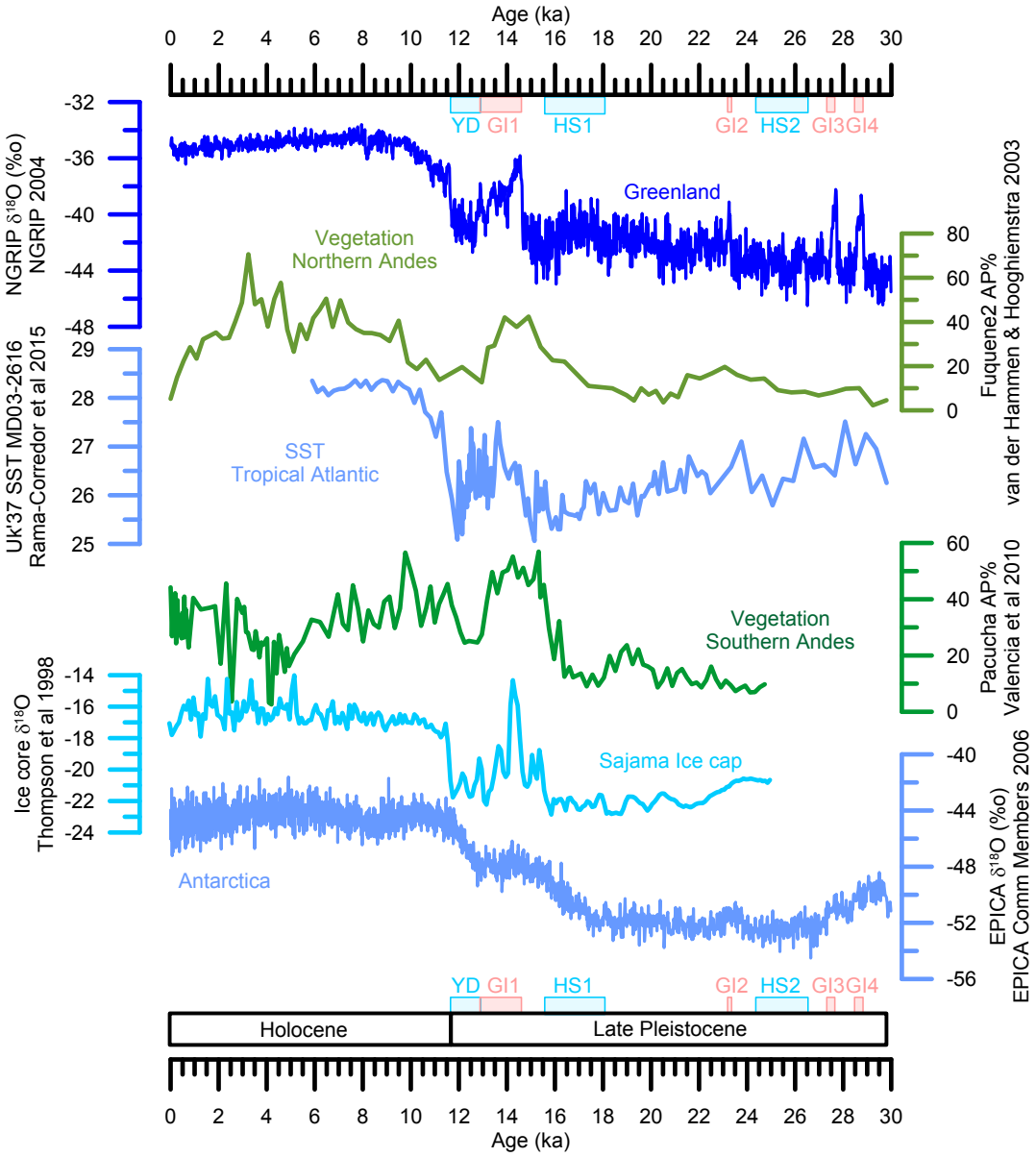

Figure 5. Millennial-scale vegetation changes in the northern and southern tropical Andes over the past 30 ka compared with other records: North Greenland (NGRIPmembers, 2004), EPICA Dome C (EPICA, 2006), and Sajama ice core record (Thompson et al., 1998), and sea surface temperatures (SST) from the Guyana Basin, tropical Atlantic (Rama-Corredor et al 2015). Heinrich stadials (HS) are drawn for reference as defined by Sánchez-Goñi & Harrison (2010). The Younger Dryas (YD) follows the timing of Greenland stadial 1 (Rasmussen et al. 2006) and the chronozone defined by Mangerud et al. (1974). The timing of Greenland interstadials (GI) is based on Wolff et al. (2010).

Table 1. Site description and details on temporal resolution and time span for eight selected pollen records in the tropical Andes. Sites are listed in a latitudinal order from North to South.

Site	Coordinates	Elevation (m asl)*	Andean position	Main moisture source	Time span (ka)	Number of ^{14}C dates	Mean temporal resolution ± SD**	Source	Latitudinal position
Llano Grande	N 06°29′ W 76°6′	3650	Inter-Andean	Atlantic ITCZ, ENSO	14	6	99±35.6	Velásquez et al. (2013)	Northern
Fúquene2	N 05°27’ W 73°46’	2540	Inter-Andean	Atlantic ITCZ, ENSO	36	10	433±167	van der Hammen & Hooghiemstra (2003)	Northern
La Cocha	N 01°06’ W 77°09’	2780	Eastern flank	Amazonian convection	14	18	26.7±16.6	González-Carranza et al. (2012)	Northern
Surucucho	S 02°51’ W 79°08’	3180	Eastern flank	Amazonian convection	21.9	9	318±175	Colinvaux et al (1997)	Central
Chochos	S 07°38’S W 77°28’	3285	Eastern flank	Amazonian convection, SASM	17.5	9	270±210	Bush et al. (2005)	Central
Pacucha	S 13°36’ W 73°19’	3050	Eastern flank	SASM, LLJ	24.9	18	198±57	Valencia et al. (2010)	Southern
Consuelo	S 13°57’ W 68°59’	1360	Eastern flank	SASM, LLJ	43.5	26	365±303	Urrego et al. (2010)	Southern
Titicaca	S 16°20’ W 65°59’	3810	Altiplano	SASM	19.7, 350	17 18	113±100, 530±720	Paduano et al. (2003), Hanselman et al. (2011)	Southern

* m asl: metres above sea level; **SD: standard deviation